A Tractography Algorithm for MR Diffusion Tensor Imaging Based on Minimum-Cost Path

C. Aronis[1], K. Delibasis[1], M. Fanariotis[2], and I. Maglogiannis[3]

[1] University of Thessaly/Department of Computer Science and Biomedical Informatics, Lamia, Greece
[2] Sykehuset Telemark HF, Skien Norway
[3] University of Piraeus/Department of Piraeus, Greece

Abstract— **Diffusion Tensor Imaging (DTI) is a powerful technique for studying tissue connectivity that starts to find routine clinical use in Magnetic Resonance Imaging (MRI), primarily in the brain. The extraction of tracts is an issue under active research. In this work we present an algorithm for recovering tracts, that is based on Dijkstra's minimum-cost path. A novel cost definition algorithm is presented that allows tract reconstruction, considering the tract's curvature, as well as its alignment with the diffusion vector field. Results are shown for two (2D) and three dimensional (3D) synthetic data, as well as for a clinical MRI-DTI brain study**

Keywords— **Diffusion Tensor Imaging (DTI), Tractography, Dijkstra's minimum-cost path.**

I. Introduction

Magnetic Resonance Diffusion Tensor Imaging (MRI – DTI) images the process of diffusion in tissue and it is clinically often applied to brain imaging [1], [2]. DTI is able to image neural fibers in white matter in the brain. Tracing image voxels with almost co-linear principal direction of diffusion is the basis for tractography (tracing fibers in MR images). Straightforward approaches like [2] have been reported. However, fiber crossing in the same image voxel, tissue regions with non-preferred direction of diffusion pose problems to tractography algorithms. A number of different approaches have been proposed to handle the aforementioned problems and better resolve fibers, using probabilistic models or non-Gaussian functions to model the orientation of diffusivity, such as Q-ball tractography, [3-5], diffusion spectral imaging [6], multiple tensor model, the CHARMED technique [7-10] or the "ball and stick" model [11]. Techniques based on spherical deconvolution [12]. Some of these approaches require high angular resolution diffusion imaging (HARDI) techniques [13].

An approach utilizing Dijkstra's shortest path algorithm has been proposed in [14]. A probabilistic shortest path approach applied to both synthetic and real data is shown in [15]. In [16], a shortest-path approach based on Gaussian process solvers of ordinary differential equations is demonstrated. Other MRI tractography algorithms that formulate the task as a Hamilton – Jacobi problem, utilize shortest-path methods [17].

In this work we present a fiber tracking algorithm that is also based on Dijkstra's shortest-path algorithm. We propose a novel cost function to assign weight to transition between image voxels that considers fiber smoothness, Euclidean distance and principal diffusion co-linearity, with variable relative weight factors, depending on the characteristics of the local diffusion tensor. Initial results are shown for synthetic two and three-dimensional data as well as clinical data.

II. Methodology

A. Basic Principles of MRI DTI

In the case of DTI, a symmetric 3x3 table **D**, called Diffusion tensor, is defined for each image voxel. The eigen-analysis of the **D** completely defines the anisotropy in water diffusion for the specific voxel. For simplicity we will not include voxel indexes in the following Equations.

$$\mathbf{D} = \begin{pmatrix} d_{11} & d_{12} & d_{13} \\ d_{12} & d_{22} & d_{23} \\ d_{13} & d_{23} & d_{33} \end{pmatrix} \quad (1)$$

For the case of anisotropy diffusion the volume is imaged using different gradient vectors $\mathbf{g}_k$ is the diffusion sensitizing gradient vectors, with k=1,2,...,N with N≥ 6. The MR signal S_i from each voxel for the ith gradient vector $\mathbf{g_i}$ is given by the following equation (originally described in [19]):

$$S_k = S_0 \cdot \mathrm{e}^{-b * \mathbf{g_k}' \cdot \mathbf{D} \cdot \mathbf{g_k}} \quad (2)$$

where S_0 is the signal intensity for the current voxel in the absence of a diffusion gradient ($\boldsymbol{g_0} = 0$), b is the diffusion weighting factor [1].

For each voxel the calculation of diffusion tensor for each voxel requires at least 6 measurements with different gradient directions (since **D** has 6 unique elements). By taking the logarithm of the above we obtain a linear system of equations:

$$\mathbf{A}.\mathbf{D}=\mathbf{S} \quad (3)$$

E. Kyriacou et al. (eds.), *XIV Mediterranean Conference on Medical and Biological Engineering and Computing 2016*,
IFMBE Proceedings 57,
DOI: 10.1007/978-3-319-32703-7_60

where $\mathbf{B} = \begin{pmatrix} d_{11} & d_{22} & d_{33} & d_{12} & d_{13} & d_{23} \end{pmatrix}^T$,

$\mathbf{S} = \left(\ln S_0 - \begin{pmatrix} \ln S_1 & \ln S_2 & \dots & \ln S_N \end{pmatrix}^T \right) / b$ and

$$A = \begin{pmatrix} x_1^2 & y_1^2 & 2x_1^2y_1^2 & 2x_1^2z_1^2 & 2y_1^2z_1^2 \\ x_2^2 & y_2^2 & 2x_2^2y_2^2 & 2x_2^2z_2^2 & 2y_2^2z_2^2 \\ \vdots & & & \vdots & \\ x_N^2 & y_N^2 & 2x_N^2y_N^2 & 2x_N^2z_N^2 & 2y_N^2z_N^2 \end{pmatrix}.$$

Eq.(3) is an over-determined system of linear equations (6 unknowns in **D** with N linear equations available). This system is easily solved:

$$\mathbf{D} = (\mathbf{A}_{6\times n}^{T} \cdot \mathbf{A}_{n\times 6})^{-1} \cdot \mathbf{A}_{6\times n}^{T} \cdot \mathbf{V}_{n\times 1} \quad (4)$$

Table **D** is calculated as aforementioned for each voxel. Thereafter, for every voxel in our data set we calculate the three eigenvectors ($\mathbf{v}_1$, $\mathbf{v}_2$, $\mathbf{v}_3$) of **D**. In the rest of this paper it is assumed that the eigenvectors are stored in descending order of the corresponding eigenvalues ($\lambda_1 > \lambda_2 > \lambda_3$).

The relation between the eigenvalues of each voxel characterizes if there is a preferred direction along which diffusion occurs. More specifically, if the largest eigenvalue (λ_1) is significantly greater than the second largest on (λ_2), then the diffusion occurs along a preferred direction, instead of it being isotropic. On the other hand, if all three eigenvalues are comparable, then diffusion occurs isotropically. If the two largest eigenvalues are similar and both are much largest than the smallest eigenvalue, then diffusion occurs predominantly along a plane (defined by $\mathbf{v_1}$ and $\mathbf{v_2}$). Linear, planar and isotropic (spherical) diffusivity is quantified by *cl*, *cp* and *cs* as it follows:

$$cl = \frac{\lambda 1 - \lambda 2}{\lambda 1}, \quad (5a)$$

$$cp = \frac{\lambda 2 - \lambda 3}{\lambda 1}, \quad (5b)$$

$$cs = \frac{\lambda 3}{\lambda 1}. \quad (5c)$$

The values of these measurements ranging from zero to one and their sum equals one:

$$cl + cp + cs = 1$$

B. The proposed DTI Tractography algorithm

The proposed algorithm uses a minimum-cost (or shortest path using an appropriate distance metric) approach to extract tracts from the vector field of the DTI. We utilize the well-known Dijkstra's algorithm. The image (2D or 3D) is considered as a directed graph G=(V,E), with each pixel/voxel being connected to all its neighbors. In 2D we employ 8-connectivity, whereas in 3D 26-voxel connectivity is considered. The algorithm is implemented similarly to its textbook version, with the following differences: A) The set of vertices S with determined distance from source is kept in a 2D/3D array. B) The distance map that holds the current estimation of the distance/cost of each voxel from the seed voxel is also a 2D/3D array with the same size as the image's. Finally two (or three in the case of 3D image) arrays of size equal to that of the image are used to store the predecessor of each pixel (voxel in 3D).

All elements of distance map array, except for a single pixel that is defined as the destination, are initialized to infinity. The cost of the destination pixel is set to 0. The arrays that hold the predecessors of the pixels in Δ are initialized to NIL.

The cost of transition between any two adjacent nodes – pixels- is calculated by considering the following factors. Let $\mathbf{p_{i-1}}$, $\mathbf{p_i}$ and $\mathbf{p_{i+1}}$ be the position vectors of the predecessor of the current pixel, the position vector of the current pixel and is the position vector of the candidate destination respectively. (Candidate destination is one of the neighboring pixels of p_i , excluding its predecessor). Similarly, let $\mathbf{V_i}$ and $\mathbf{V_{i+1}}$ be the corresponding eigenvectors (of the current and candidate destination voxel) with the largest eigenvalue and cl_i be the linear diffusivity of the corresponding pixel $\mathbf{p_i}$. We calculate the angle θ_1 between ($\mathbf{p_i}$ -$\mathbf{p_{i-1}}$) and ($\mathbf{p_{i+1}}$ - $\mathbf{p_i}$), as shown in Fig. 1. Thus, the first term of the cost function is defined as $F_1 = (cos\theta_1 + 1)$. Minimization of this term favors smooth curves.

The second term is defined as: $F_2 = (1 - |cos\theta_2|)$, where θ_2 is the angle between (p_{i+1} - p_i) and V_i . Thus minimization of this term favors the local transition from p_i to p_{i+1} , which is almost parallel to eigenvector V_i of the current node p_i .The absolute value | |, is inserted because both directions of V_i may be selected.

The third term is defined as $F_3 = (|cos\theta_3| + 1)$, where θ_3 is the angle between V_i and V_{i+1}. This term favors transitions to a neighboring pixel with eigenvector V_{i+1} that is almost parallel to eigenvector V_i.

We combine the three mentioned terms by adding them use these calculations by summarize them in the following equation:

$$(cos\theta_1 + 1) + (1 - |cos\theta_2|) + (1 - |cos\theta_3|) \quad (6)$$

We rely heavily on the above distance (cost) metric for pixels with high linear diffusivity measure (*cl*) as defined in Eq.(5a). In the case of current voxel with low coefficient of linear diffusivity, we use primarily the Euclidean distance of the transition from current voxel to the candidate destination. Thus, the cost d_{i+1} (distance metric) of the transition from p_i to p_{i+1} is defined as the weighted average of the

expression in (6) and the Euclidean distance of the transition $\|p_{i+1} - p_i\|$ as follows:

$$d_{i+1} = \left((\cos\theta_1 + 1) + \left(1 - |\cos\theta_2|\right) + \left(1 - |\cos\theta_3|\right)\right) cl_i + \|\mathbf{p}_{i+1} - \mathbf{p}_i\| cl_i \quad (7)$$

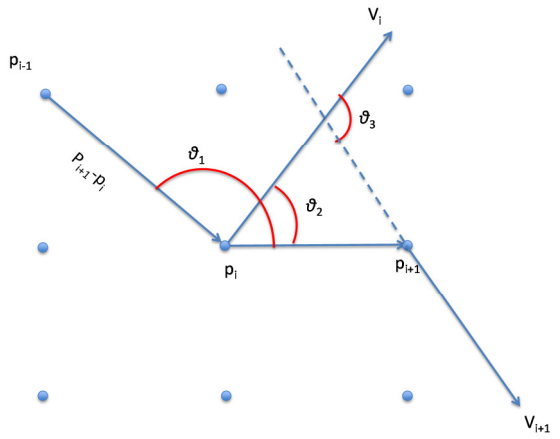

Fig. 1. The concept of calculating the cost of moving from pixel $\mathbf{p_i}$ to $\mathbf{p_{i+1}}$, given the predecessor of $\mathbf{p_i}$ and the largest eigenvectors of $\mathbf{p_i}$ and $\mathbf{p_{i+1}}$.

III. RESULTS

A. Synthetic and real data

In order to quantify the accuracy of the algorithm we generated synthetic data as following. A 2D domain $D = [-2,2] \times [-2,2] \subset \Re^2$ was arbitrarily defined. Domain D was discretized to produce pixels of size (δx, δy). Let us call the discrete domain Δ. Thus the center of Δ_{ij} equals $(-2 + j + \delta x/2, -2 + i + \delta y/2)$.

A continuous curve $\mathbf{c}(t) = (x(t), y(t))$ representing the tract (to be discovered) was selected inside *D*, using b-spline interpolation over a number of arbitrarily selected points. Thus $\mathbf{c}(t)$ is known in advance and will be used for ground truth. The proposed tracking algorithm uses the principal eigenvector at each pixel, as well as the linear diffusivity –defined Eq.(5a). Let $\mathbf{v_1}(i,j)=(v_x(i,j), v_y(i,j))$ be the principal eigenvector of $\mathbf{c}(t)$ at pixel (i,j) of Δ. In the synthetic data, the principal eigenvectors were simulated as following. Curve $\mathbf{c}(t)$ is discretized by varying its parameter t by a small step δt (we will refer to the discrete curve as c[t]). $\mathbf{v_1}(i,j)$ is initialized as (0,0) for each (i,j) in Δ. For each point of $\mathbf{c}[t]$, the closest pixel (i,j) of Δ is located and the corresponding principal eigenvector was set as the unit-length tangent vector of c[t]:

$$\mathbf{v}(i,j) = \left(v_x(i,j), v_y(i,j)\right) = \dot{\mathbf{c}}[t] / \left\|\dot{\mathbf{c}}[t]\right\| = \left(\dot{x}[t], \dot{y}[t]\right) / \left\|\left(\dot{x}[t], \dot{y}[t]\right)\right\|, \quad \dot{\mathbf{c}}[t] = \dot{\mathbf{c}}[t + \delta t] - \dot{\mathbf{c}}[t] \quad (6)$$

An inpainting algorithm was employed to fill the rest of the pixels of Δ by cascading *K* times the linear convolution operator of the *X* and *Y* components of **v** with a 3x3 mask *M* [18], thus inducing isotropic diffusion of the initial eigenvectors across the pixels of Δ.

```
for k=1 to K {
    v_x = v_x * M;
    v_y = v_y * M;
}
```

where *M* is defined as

$$M = \begin{pmatrix} c & c & c \\ c & 0 & c \\ c & c & c \end{pmatrix}, c = 1/8 \quad (7)$$

Fig. 2 shows the ground truth track superimposed on the vector field that will be used as the primary eigenvector in our tractography experiments with synthetic data. The length of the vectors is used to emulate the linear diffusivity factor *cl* in a real DTI study.

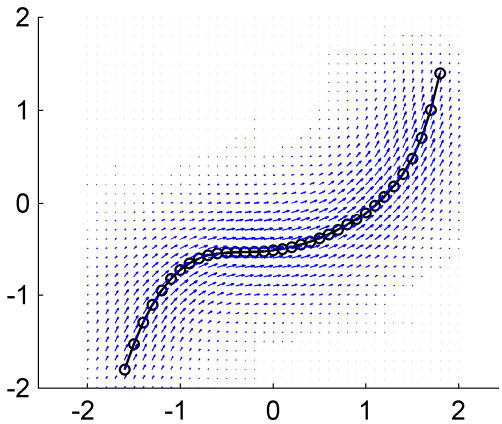

Fig. 2 The artificial fiber and the primary vectors according to Eq. (4). The length of the vectors represents the linear diffusivity factor *cl* Eq. (5a).

More than one artificial tracts can be defined and the relevant vector field (with the diffusivity factor *cl*) may be generated by simple vector/algebraic addition. Fig. 3 shows two fibers (tracts) and the corresponding vector field. This image is also used in this work to test the ability of the proposed algorithm to track crossing tracts.

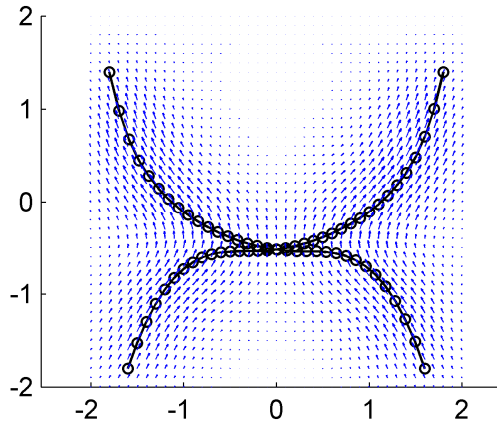

Fig. 3. Two artificial fibers (racks) and the primary vectors according to Eq.(6). The length of the vectors represents the linear diffusivity factor *cl*.

Synthetic data are also generated in three dimensions (3D) by generalizing the aforementioned process. A number of experiments were conducted for 1 and 2 tracts, using different pixilations of the Δ image domain. Similarly, experiments with different number of voxels were carried out in 3D synthetic data. For low resolution data (64x64x32) the proposed algorithm requires approx. 4 minutes on an average laptop using Matlab.

Real data consist of an anonymous clinical brain DTI study using 32 different gradients, each of which imaged 27 transverse slices of 256x256 pixels, at different gradient vectors. The data were provides by the Dept. of Medicine, University of Thessaly.

B. Quantitative results

The positional error of the tract determined by the proposed algorithm was quantified as following. A binary image B of size equal to image domain Δ is initialized to 0. The pixels of the discretized ground truth tract $\mathbf{c}[t]$ in image *B* are set to 1. The distance transform (*DT*) of B is calculated. Finally, the positional error (*err*) is calculated as the mean value of the pixels determined by the proposed tracking algorithm $\mathbf{q}(n)$, n=1,2, …

$$err = \frac{1}{L}\sum_{n} I\left(\mathbf{q}(n)\right), I = DT\left(B\left(c[t]\right)\right) \qquad (8)$$

Units of error are in pixels, thus average positional error below 1 indicates subpixel accuracy.

Table I shows the mean positional error achieved by the proposed algorithm, for several tracking experiments of synthetic fibers in 2 and 3 dimensions. In case of more than one existing fiber, the following symbols are used in column 3: U: upper, D: down, R: right. L: left.

Table 1 Average positional error (in pixels) of the proposed tractography algorithm for several experimental setups.

Experiment	Domain pixilation	Fibers	Average positional error (pixels)
Synthetic 2D, 1 tract	32×32	1	0.15
	41×41	1	0.22
	64×64	1	0.40
	128×128	1	0.42
Synthetic 2D, 2 tracts	32×32	UL→DR	0.25
	64×64	UL→DR	0.32
	128×128	UL→DR	0.38
	32×32	DL→UR	0.38
	64×64	DL→UR	0.79
	128×128	DL→UR	0.49
Synthetic 3D, 1 tract	16×16×16	1	2.25
	32×32×32	1	2.15

The tract found by the proposed algorithm for the 2D single tract synthetic data are shown in Fig. 4 for two different pixilations of Δ: 32×32 (a) and 128×128 (b). Filled circle denotes destination point, star denotes starting pixel. The ground truth fiber (dark thick curve) is also shown. Fig. 5 presents the resulting tract for the 2D synthetic data that contain 2 intersecting tracts, with 64×64 size of the discrete domain Δ.

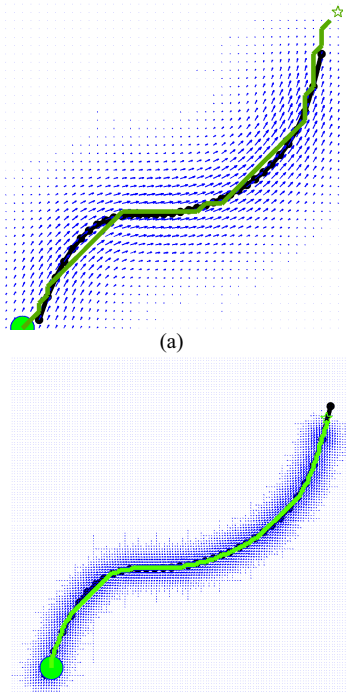

(a)

(b)

Fig. 4. The resulting tract (green thick curve) of the proposed algorithm for synthetic 2D image with 1 fiber. Filled circle denotes destination point,

star –upper right- denotes starting pixel. The ground truth fiber (dark thick curve is also shown).

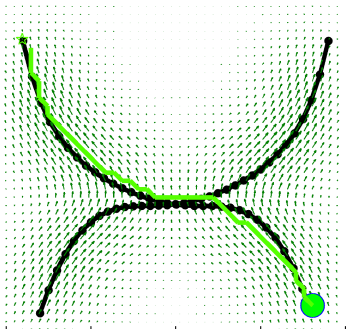

Fig. 5. The resulting tract (green thick curve) generated by the proposed algorithm (filled circle denotes destination point, star –upper right- denotes starting pixel). The ground truth tract (dark thick curve is also shown).

Fig. 6 shows the resulting tract for the 3D synthetic data (that contain a single tract), with 32×32×32 size of the discrete domain Δ. The accuracy of the tracking process may be assessed visually. It is also quantified in Table 1.

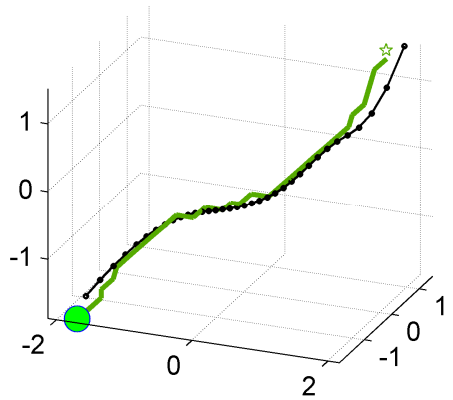

Fig. 6. The resulting tract (green thick curve) of the proposed algorithm in the case of 3D synthetic data of resolution 32x32x32. Filled circle denotes destination point, star –upper right- denotes starting pixel. The ground truth tract (dark thick curve) is also shown.

The proposed algorithm was also applied to clinical MDI-DTI. The resulting fibers for two well-known exiting neural paths, are shown in Fig. 7. Starting and ending voxels are indicated by a star and a circle respectively. The primary vectors are also shown for pixels with high linear diffusivity *cl*.

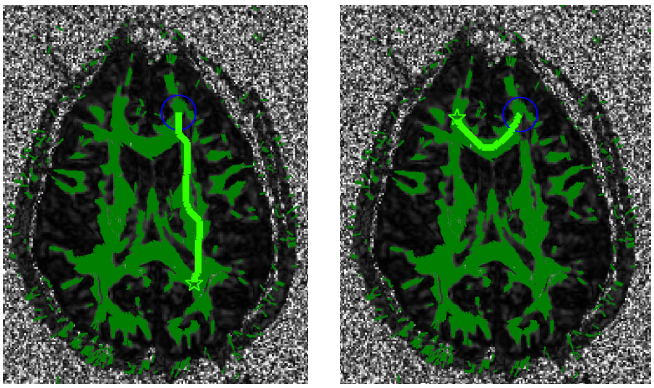

(a) (b)

Fig. 7. The resulting fiber (green thick curve) generated by the proposed algorithm (filled circle denotes destination point, star –upper right- denotes starting pixel). The ground truth tract (dark thick curve is also shown)

The details of fiber tracking in real MRI-DTI data are shown in Fig. 8. The resulting fibers appear visually plausible, in accordance to the definition of the cost function and appear to agree with physiology.

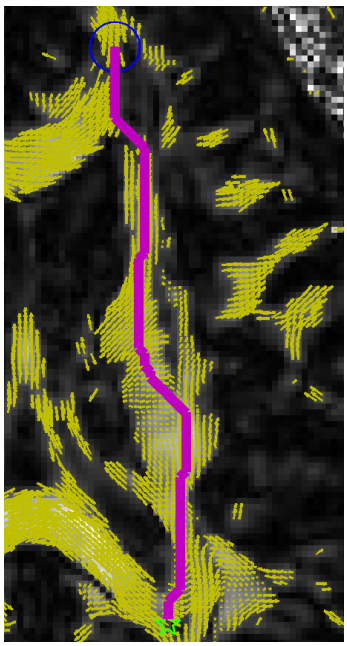

(a)

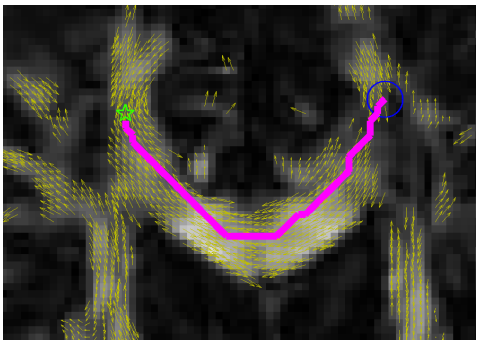

(b)

Fig. 8. Details of fiber tracking of Fig. 7.

IV. Conclusions

An algorithm for tracing fibers in MRI DTI studies has been presented. The proposed algorithm is based on Dijkstra's shortest path and uses a suitably defined cost function to calculate the cost of transition between neighboring voxels. Results on synthetic 2D tensor fields show sub-pixel accuracy, even in cases of intersecting fibers. Initial results from 3D tensor fields (emulating MRI-DTI data) show average positional error of approx. 2.5 voxels. When applied to real brain MRI-DTI studies, the proposed algorithm identified well known neural tracks.

Conflict of Interest

"The authors declare that they have no conflict of interest".

References

1. Le Bihan, D., Mangin, J. F., Poupon, C., Clark, C. A., Pappata, S., Molko, N., & Chabriat, H. (2001). Diffusion tensor imaging: concepts and applications. Journal of magnetic resonance imaging, 13(4), 534-546.
2. Westin, C. F., Maier, S. E., Mamata, H., Nabavi, A., Jolesz, F. A., & Kikinis, R. (2002). Processing and visualization for diffusion tensor MRI. Medical image analysis, 6(2): 93-108
3. Tuch D S. (2004) Q-ball imaging. Magn Res Med, 52:1358-1372.
4. Descoteaux, M., & Deriche, R. (2015). From Local Q-Ball Estimation to Fibre Crossing Tractography. In Handbook of Biomedical Imaging (pp. 455-473). Springer US.
5. Descoteaux, M., Deriche, R., Le Bihan, D., Mangin, J. F., & Poupon, C. (2011). Multiple q-shell diffusion propagator imaging. Medical image analysis, 15(4), 603-621.
6. Wedeen V J, Reese T, Tuch D S, Weigel M, Dou J-G, et al. (2000) Mapping fiber orientation spectra in cerebral white matter with fourier-transform diffusion MRI. In Proc Intl Soc Mag Reson Med, 8.
7. Pasternak O, Assaf Y, Intratora N, and Sochen N. (2008). Variational multiple-tensor fitting of fiber-ambiguous di usion-weighted magnetic resonance imaging voxels. Magn Reson Med, 26:1133-1144.
8. Tournier J D, Yeh C-H, Calamante F, Cho K-H, Connelly A, et al. (2008) Resolving crossing fibers using constrained spherical deconvolution: validation using diffusion weighted imaging phantom data. Neuroimage, 42:617-625.
9. Assaf Y. and Basser P. J. Composite hindered and restricted model of diffusion (CHARMED) MR imaging of the human brain. Neuroimage, 27:48{58, 2005
10. Zhang, F., Hancock, E.R., Goodlett, C., Gerig, G. (2009) Probabilistic white matter fiber tracking using particle filtering and von Mises-Fisher sampling. MedIA 13(1) :5–18
11. Behrens T E J, Johansen-Berg H, Jbabdi S, Rushworth M F S, and Woolrich M W, (2007), Probabilistic diffusion tractography with multiple fibre orientations. what can we gain? NeuroImage, 34(1):144–155.
12. A. Anwander, M. Tittgemeyer, D. Y. von Cramon, A. D. Friederici and T. R. Knosche (2007) Connectivity-based parcellation of broca's area. Cerebral Cortex, 17(4):816–825.
13. D. Alexander. An Introduction to Diffusion MRI: the Diffusion Tensor and Beyond. Springer, 2006
14. Henry, R. G., Shieh, M., Amirbekian, B., Chung, S., Okuda, D. T., & Pelletier, D. (2009). Connecting white matter injury and thalamic atrophy in clinically isolated syndromes. Journal of the neurological sciences, 282(1), 61-66.
15. Zalesky, A. (2008). DT-MRI fiber tracking: a shortest paths approach. Medical Imaging, IEEE Transactions on, 27(10), 1458-1471
16. Schober, M., Kasenburg, N., Feragen, A., Hennig, P., & Hauberg, S. (2014). Probabilistic shortest path tractography in DTI using Gaussian Process ODE solvers. In Medical Image Computing and Computer-Assisted Intervention–MICCAI 2014 (pp. 265-272). Springer International Publishing.
17. Jeong, W. K., Fletcher, P. T., Tao, R., & Whitaker, R. T. (2007). Interactive visualization of volumetric white matter connectivity in DT-MRI using a parallel-hardware Hamilton-Jacobi solver. Visualization and Computer Graphics, IEEE Transactions on, 13(6):1480-1487.
18. Richard, M. M. O. B. B., & Chang, M. Y. S. (2001). Fast digital image inpainting. In Appeared in the Proceedings of the International Conference on Visualization, Imaging and Image Processing (VIIP 2001), Marbella, Spain, pp. 106-107.
19. Stejskal, E. O., & Tanner, J. E. (1965). Spin diffusion measurements: spin echoes in the presence of a time-dependent field gradient. The journal of chemical physics, 42(1), 288-292.

Use macro [author address] to enter the address of the corresponding author:
Author: Ilias Maglogiannis
Institute: University of Piraeus
Street: Grigoriou Lampraki 126
City: Piraeus
Country: Greece
Email: imaglo@unipi.gr